Transient Kinetic Analysis of *N*-Phenylmaleimide-Reacted Myosin Subfragment-1

Ling Xie,[‡] Wan Xia Li,[‡] Troy Rhodes,[§] Howard White,[§] and Mark Schoenberg*,[‡]

National Institute of Arthritis and Musculoskeletal and Skin Diseases, National Institutes of Health, Bethesda, Maryland 20892, and Department of Pharmacology, Physiology, and Biochemistry, Eastern Virginia Medical School, Norfolk, Virginia 23507

Received July 23, 1998; Revised Manuscript Received March 9, 1999

ABSTRACT: Alkylation of myosin's Cys-707 (SH1) and Cys-697 (SH2) has profound consequences for myosin's ability to interact with actin and hydrolyze MgATP. Pre-steady-state measurements of myosin-S1 alkylated at SH1 and SH2 by *N*-phenylmaleimide (NPM) in the presence of ATP were taken to identify the steps of the reaction that are altered. It was found that the rate constant most affected by this modification is the apparent rate of the ATP hydrolysis step. This rate constant is reduced 20000-fold, an effect comparable in magnitude to the effect of the same modification on the binding of MgATP to S1 or acto-S1 [Xie, L., and Schoenberg, M. (1998) *Biochemistry 37,* 8048]. In contrast, the rate constants of phosphate release and dissociation of acto-S1 by ATP were reduced <20-fold. For unmodified S1, the enhancement of fluorescence seen after addition of ATP had the same rate constant as the ATP hydrolysis step (S1·ATP ⇔ S1·ADP·P_i) measured by single-turnover experiments in a quench-flow experiment. This is consistent with results previously observed [Johnson, K. A., and Taylor, E. W. (1978) Biochemistry *17,* 3432]. However, NPM-modified S1 exhibited virtually no fluorescence enhancement upon ATP binding. This provides further evidence that M·ATP is the predominant intermediate of NPM−S1-catalyzed ATP hydrolysis.

A critical feature of the chemomechanical coupling of myosin motor function is the cyclic association and dissociation of the myosin molecule and the F-actin molecule during the hydrolysis of ATP, which leads to the movement of actin filaments in cells. ATP hydrolysis by actomyosin can be explained by the following mechanism.

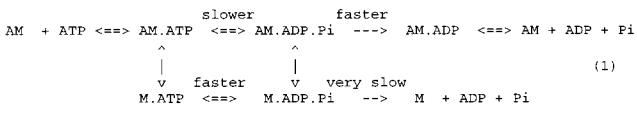

The following features are key aspects of this mechanism. (1) Actomyosin is rapidly dissociated upon ATP binding to myosin, which is followed by a rapid hydrolysis of ATP. (2) Product release, which is rate-limiting, is significantly accelerated by actin binding.

In the normal actomyosin ATP hydrolysis cycle, myosin alternates between its weakly and strongly binding conformations (*1*, *2*). Both *N*-phenylmaleimide (NPM) and *p*-phenylenedimaleimide (pPDM) interact with the essential sulfhydryls of myosin (SH1 and SH2) and greatly inhibit the ability of myosin to hydrolyze ATP (*3*−6). pPDM-reacted myosin subfragment-1 is locked in a weakly binding conformation (*7*, *8*), suggesting a possible mechanism for its inhibition of ATP hydrolysis. However, NPM−S1 is not locked in a weakly binding conformation (*8*, *9*), and the mechanism by which NPM modification inhibits ATP hydrolysis is unclear. In the work described here, we used stopped-flow and quench-flow measurements to determine the detailed hydrolysis mechanism of NPM-modified S1.

From equilibrium binding data, Xie and Schoenberg (*8*) found that NPM modification has relatively little effect on the binding of myosin to actin. Although that work also revealed that modification by NPM decreases the affinity of ATP for the active site of myosin, it does not explain why NPM modification has such a large effect on ATPase activity. The current work reveals that NPM modification of SH1 and SH2 inhibits ATP hydrolysis by causing a very large reduction in the apparent rate constant of the hydrolytic step.

MATERIALS AND METHODS

Reagents. NPM was obtained from Aldrich Chemical Co. (Milwaukee, WI) and dissolved in dimethylformamide to a final concentration of 50 mM. Dithiothreitol (DTT) was obtained from ICN Biochemicals (Aurora, OH), and ATP and ADP were obtained from Sigma (St. Louis, MO). 1-N^6-Etheno-2-aza-ATP was synthesized as described by Smith and White (*10*).

Proteins. Rabbit skeletal myosin subfragment-1 was prepared by chymotryptic digestion of myosin as previously described (*11*). The preparation of NPM−S1 was like that described by Xie and Schoenberg (*8*). F-Actin was made according to the procedure of Pardee and Spudich (*12*). It was stored in 100 mM KCl, 3 mM $MgCl_2$, 0.0005% NaN_3, and 10 mM imidazole (pH 7.0).

The molecular masses for S1 and actin were taken to be 120 and 42 kDa, respectively. The extinction coefficients ($A^{1\%}$) at 280 nm were 7.5 cm^{-1} for S1 and 11 cm^{-1} for actin. The concentration of NPM−S1 was determined with a Lowry assay (*13*).

* To whom correspondence should be addressed: NIH Bldg. 6, Rm. 408, Bethesda, MD 20892. E-mail: mark@lpb.niams.nih.gov. Phone: (301) 496-1023. Fax: (301) 480-1026.

[‡] National Institutes of Health.

[§] Eastern Virginia Medical School.

10.1021/bi981778o CCC: $18.00
Published on Web 04/14/1999

Single-Turnover Quench-Flow Experiments. Chemical quench measurements were taken using a computer-controlled stepper motor-driven quench-flow apparatus. Syringes of the quench-flow sample handling unit (model 27001, Kintek Corp., State College, PA) were driven by a 34A109E stepper motor (Anaheim Automation, Anaheim, CA) which was powered by an IMS Panther HI2 microstepper motor controller (Servo-Systems, Montville, NJ). A program written in turbo basic and running on a Zenith 140 personal computer provided the timing. Solutions of myosin-S1 (20 μL) and ATP (15 μL) containing 10000−20000 dpm of [^{32}P]ATP (Dupont, BLU-002) were loaded into the sample loops of the model 27001 instrument and driven into a delay line by buffer from the drive syringes. After incubation for the desired amount of time, a second drive was used to expel the reaction mixture and quench it with acid (0.35 M KH_2PO_4 in 2 N HCl) to give a final sample volume of 1.0 mL. Reaction times down to 100 ms could be obtained using this configuration. Reaction times of less than 100 ms were obtained by using the quench-flow apparatus in a single-push mode in which the time was varied by the length of the delay line and the velocity of the flow. A 0.4 mL portion of the quenched sample was mixed with an equal volume of a 10% slurry of activated charcoal (Sigma, C-4386) under acid quench conditions and centrifuged to remove unhydrolyzed ATP. Control experiments indicated that more than 99% of the unhydrolyzed ATP is bound to charcoal. The amount of total radioactivity of ATP in each sample was determined by counting 0.2 mL directly. The percent hydrolysis was obtained from the ratio of the radioactivity in charcoal-treated to directly counted samples after subtracting background from each.

In the single-turnover quench-flow experiments, concentrations were chosen such that [S1] > [ATP]. Single- or double-exponential equations were fit to the data using a least-squares fitting routine based upon Marquardt's compromise (*14*) to determine the rate constant and amplitudes of the hydrolysis reaction.

Steady-State ATP Hydrolysis. The rate constants for steady-state ATP hydrolysis were obtained by determining the amount of phosphate liberated from [γ-^{32}P]ATP in a manner similar to that described above. The steady-state measurements (as well as the long time-scale single-turnover measurements for NPM−S1) were taken in 1.5 mL Eppendorf tubes with 0.5 mL reaction volumes.

Each assay contained 1−100 μM myosin subfragment-1 in 0.49 mL of buffer which contained 5 mM MOPS, 2 mM $MgCl_2$, and 0.2 mM DTT. Controls contained only buffer. To begin the reaction, 0.01 mL of 0.125−2.5 mM [γ-^{32}P]-ATP was added to the reaction and control tubes. At the desired times, an aliquot of 0.02 mL was taken from the incubation tube and added to 0.5 mL of "quench buffer" containing 0.35 M monobasic sodium phosphate in 2 N HCl to stop the reaction. The mixture (0.15 mL) in the quench tube was removed and the amount of total radioactivity counted. Another 0.3 mL of mixture in the quench tube was removed and mixed with 0.3 mL of 10% charcoal in quench buffer. The charcoal mixture was spun for 5 min at 10 000 rpm, after which 0.3 mL of the supernatant was assessed for free P_i content. The fraction of ATP hydrolysis, F, was calculated as follows:

$$F = \frac{\text{supernatant counts in S1 tube} - \text{supernatant counts in control tube}}{\text{total counts in S1 tube} - \text{supernatant counts in control tube}}$$

The steady-state rate constant measurements were taken using 1 μM S1 and 50 μM ATP. The rate constant for steady-state ATP hydrolysis was determined from the slope of the best straight-line fit to the data × [ATP]/[S1]. In some instances, steady-state rate constants also were measured in the quench-flow apparatus and gave results similar to those obtained by manual methods.

Stopped-Flow Measurements of Tryptophan Fluorescence Enhancement and Dissociation of Actomyosin by ATP. Stopped-flow measurements of tryptophan fluorescence enhancement were taken as described previously (*15*). Myosin-S1 was mixed with MgATP in a stopped-flow fluorimeter. The observed increases in tryptophan fluorescence were fit to a single-exponential equation by the method of moments (*16*).

Acto-S1 dissociation measurements were taken in the same buffer as the ATPase measurements, using light scattering to measure dissociation. Steady-state fluorescence spectra were recorded with an Aminco-Bowman Series 2 spectrofluorimeter (Spectronic Instruments, Inc., Germantown, MD).

Cold-Quench Experiments. Two kinds of cold-quench experiments were performed. In one kind, 40 μM [γ-^{32}P]-ATP was mixed, at time zero, with 20 μM S1 in the quench-flow apparatus described above. After the indicated time, cold ATP was added to give a concentration of 5 mM in the reaction mixture to prevent any more binding of [γ-^{32}P]ATP to myosin-S1. Subsequently, the mixture was allowed to incubate for 20 min to allow all bound [γ-^{32}P]ATP to be hydrolyzed before stopping the reaction by adding quench buffer. The amount of P_i that was liberated was determined as described above. Initial binding and hydrolysis after the addition of cold ATP both took place at 20 °C. This type of experiment was used to determine the kinetics of irreversible ATP binding to the active site.

In the second kind of cold-quench experiment, the [γ-^{32}P]-ATP was allowed to bind for 2−3 s to the NPM−S1 and cold ATP was added to give a concentration of 5 mM. The time between the cold quench and the acid quench was then varied between 10 and 300 s. This type of experiment measures the rate of breakdown of the tightly bound M·ATP to products.

RESULTS

MgATP Dissociation of S1 from Actin. It previously was shown that the equilibrium constant for MgATP binding to acto-S1 is reduced nearly 10000-fold by NPM reaction of the SH1 and SH2 sulfhydryls (*8*). If this effect is due to an effect on the forward rate constant for ATP binding, it should lead to a very large decrease in the rate constant with which ATP dissociates S1 from actin.

Typical light scattering records for unmodified and NPM−S1 are shown in panels A and B of Figure 1, respectively. The rates of dissociation of unmodified and NPM−S1 by ATP were measured from the decrease in light scattering observed in a stopped-flow fluorimeter. The solid lines through the data are the best fits of single-exponential equations to the data. Single-exponential fits give a reasonable, but clearly not perfect, fit to the data for unmodified

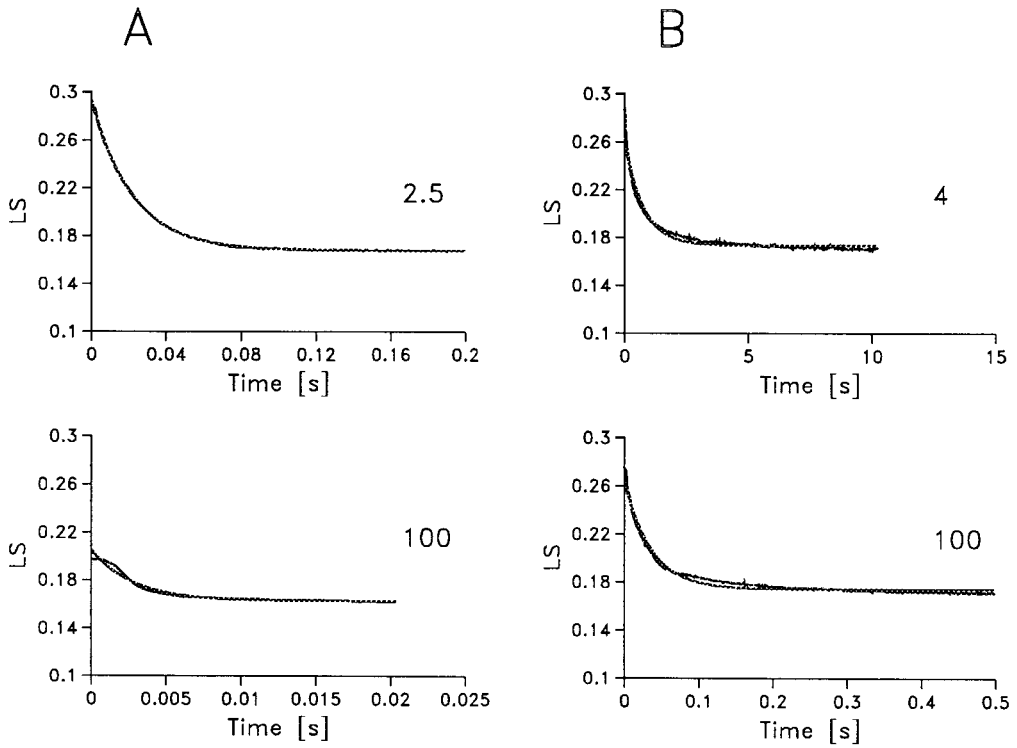

FIGURE 1: Typical light scattering records observed upon mixing for unmodified (A) and NPM-reacted (B) actomyosin-S1 with equal volumes of MgATP in a stopped-flow fluorimeter. Final concentrations were 1.5 μM actin and 1 μM S1 in a buffer containing 2 mM $MgCl_2$, 0.2 mM DTT, and 5 mM MOPS at 20 °C. Final ATP concentrations are given next to each trace in millimolar. Solid lines are single-exponential fits to the data.

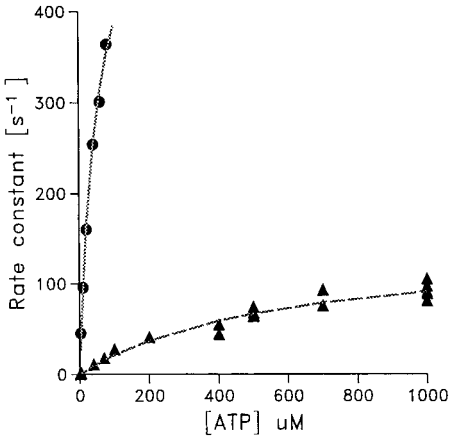

FIGURE 2: Rate constant for the light scattering change as a function of ATP concentration for unmodified (●) and NPM−S1 (▲).

S1 at low ATP concentrations. At high ATP concentrations with unmodified S1, there is a lag in the response, the amplitude is diminished, and the curve clearly is not fit by a single-exponential equation. This is because the duration of the dissociation is on the same time scale as the mixing time of the stopped-flow apparatus. Such nonexponential data were not analyzed further and are not included in Figure 2.

Figure 2 shows the dependence of the rate constant for the light scattering change upon ATP concentration for both unmodified and NPM−S1. The initial slope of the plot, the apparent second-order rate constant of the dissociation of S1 from actin by MgATP, is reduced ~16-fold by NPM modification of the SH1 and SH2 sulfhydryls. The relatively small decrease in the observed rate of dissociation indicates that most of the 10^4-fold decrease in the binding affinity of ATP for acto-NPM−S1 caused by NPM modification (*8*) must be from an ~600-fold increase in the rate of dissociation of ATP from acto-NPM−S1.

Hydrolysis Rate Constants. For unmodified myosin-S1, the rate-limiting step in the ATP hydrolysis mechanism is either P_i release or a step just before it (*1*, *17*). The rate constant for P_i release is equal to the steady-state rate of P_i liberation, and the rate constant for ATP hydrolysis can be measured by quenching the hydrolysis reaction with acid at different time intervals in a single-turnover experiment.

Panels A and B of Figure 3 illustrate the data from single-turnover experiments for unmodified and NPM−S1, respectively. The single-turnover rate for the hydrolysis of ATP by NPM−S1 is independent of concentration over the experimentally accessible range (1−75 μM), indicating that substrate binding is not rate-limiting. The ATPase rate constants, *k*, for the single-turnover experiments whose data are depicted in Figure 3, were determined directly from a fit of the equation $F = F_o[1 - \exp(-kt)]$ to the data. F_o is the final fraction of P_i hydrolyzed, and *k* is the rate constant of hydrolysis.

The values of the rate constants for single-turnover ATP hydrolysis, as well as those for steady-state hydrolysis, along with 95% confidence limits are shown in Table 1. For unmodified S1, the maximum rate of 72 s^{-1} in the single-turnover experiment is more than 1000 times faster than the steady-state rate (0.064 s^{-1}). For the NPM-modified S1, the rate constant for the single-turnover experiment is decreased 20000-fold and is equal to the steady-state rate constant (0.003 s^{-1}).

The lack of spectroscopic signals associated with the product dissociation steps makes it difficult to measure the kinetics of these steps for NPM−S1. Single-turnover experiments were therefore carried out in the presence of ADP to

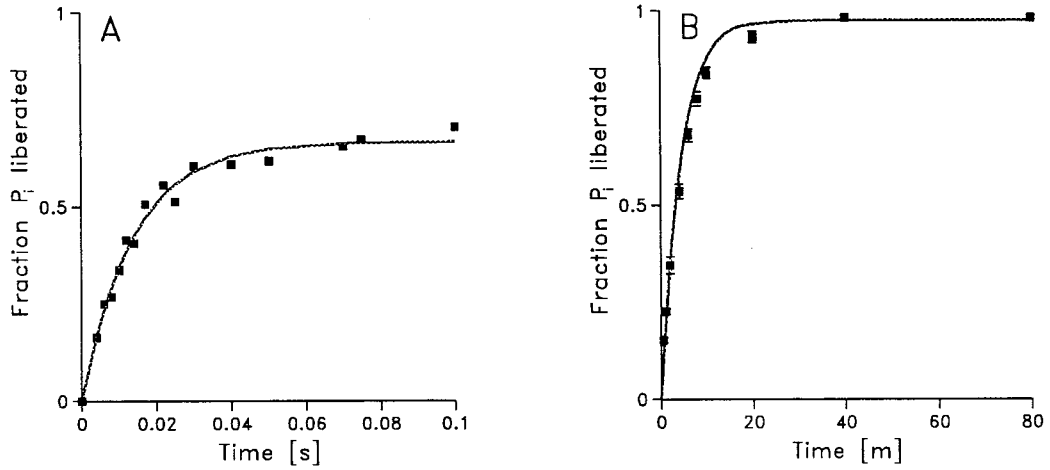

FIGURE 3: Single-turnover hydrolysis. Buffer conditions are the same as those described in the legend of Figure 1. (A) Equal volumes of 150 μM unmodified S1 and 15 μM ATP were mixed using a quench-flow apparatus as described in Materials and Methods and quenched with acid at the indicated time. (B) Time course of P_i liberation with 100 μM NPM−S1 and 50 μM ATP ($n = 4$) as described in Materials and Methods. Note the vastly different time scales in panels A and B.

Table 1: ATPase Rate Constants (s^{-1})

experiment	control	NPM-reacted
single-turnover	72	0.0038 ± 0.0004
steady-state	0.064 ± 0.007	0.0030 ± 0.0001

obtain an estimate of the affinity of ADP for NPM−S1. ADP inhibits the rate of single-turnover ATP hydrolysis with an apparent dissociation constant of 0.55 mM for NPM−S1 compared to 1−2 μM for unmodified S1. These data indicate a 250−500-fold reduction in the affinity of NPM−S1 for ADP relative to that of unmodified S1.

Cold-Quench Experiments. The simplest interpretation of our steady-state ATPase measurements is that NPM−S1 hydrolyzes ATP at a slow but non-zero rate of $\sim$0.003 s^{-1}. An alternative explanation is that NPM−S1 ATP hydrolysis is completely inhibited and the slow ATPase activity of the NPM-reacted preparation is due to a small amount of contaminating unreacted S1 hydrolyzing ATP at the normal rate. Cold-quench experiments distinguish between these possibilities by measuring the fraction of myosin capable of tightly binding ATP and the rate at which the bound ATP is hydrolyzed.

Steady-state rate measurements of ATP hydrolysis by NPM−S1 are about 5% of that of unmodified S1 (Table 1). If the slow rate of hydrolysis was due to a small amount of unmodified S1 hydrolyzing ATP at the normal rate, then, at the time when cold ATP is added to the reaction mixture in the cold-quench experiment, no more than 5% of the protein would have nucleotide tightly bound. In three separate cold-quench experiments (data from one example are shown in Figure 4A), much larger fractions of myosin-S1 were found to be capable of ATP binding and hydrolysis. An apparent burst, corresponding to approximately 20% of the myosin sites, irreversibly bound ATP and eventually hydrolyzed it. The fraction of sites producing products in the cold-quench experiment is too large for a fraction of unmodified S1 to account for the steady-state rate. It is, however, much less than that observed for unmodified myosin in which the partition of bound ATP is almost all toward products.

The reduction in the size of the cold-quench burst for NPM-modified myosin is explained by the partitioning of the bound nucleotide between products and ATP, which is a measure of the ratio between the rate of release of products into solution and the rate of dissociation of ATP. This provides an estimate of $0.003/0.2 \approx 0.015$ s^{-1} for the rate constant of ATP dissociation from NPM-modified S1. These data are consistent with NPM-modified S1 having an ATPase rate that is reduced 20-fold and a substrate affinity that is several orders of magnitude lower than that of unmodified S1.

Stopped-Flow and Steady-State Fluorescence Measurements. It previously has been observed that the rate of intrinsic tryptophan fluorescence enhancement at a saturating ATP concentration is similar to the rate of the bond-splitting step ($M{\cdot}ATP \Leftrightarrow M{\cdot}ADP{\cdot}P_i$) (*18*). Such experiments are technically quite difficult, and it is possible that the equality between the rates of the fluorescence change and the hydrolysis rate could fortuitously depend on experimental conditions. We therefore thought it was worthwhile to repeat these experiments. We found that the saturating value for the fluorescence change rate constant (74 ± 2, Figure 5) is very similar to the maximum value of 72 s^{-1} measured in the single-turnover quench-flow experiments for unmodified S1. These results are consistent with previous conclusions that either a conformational change limits the rate of the hydrolysis step or there is tight coupling between the conformation change and hydrolysis (*18*).

No fluorescence change was observed upon mixing ATP with NPM−S1 in the stopped-flow apparatus. This suggested that the fluorescence change seen on MgATP binding either was absent in NPM−S1 or occurred too slowly to be detected. To distinguish between these possibilities, we measured the steady-state intrinsic tryptophan fluorescence of unreacted and NPM−S1 in a spectrofluorimeter. The intrinsic fluorescence of NPM−S1 in rigor solution was close to that of control S1. However, the intrinsic fluorescence of control S1 changed $\sim$20% on MgATP binding, while that of NPM−S1 changed only 1.3 ± 2%. From this and equilibrium binding data (*8*), it is clear that MgATP binds to both control and NPM−S1, but NPM−S1 does not exhibit a significant fluorescence increase.

Aza-ATP Binding. Stopped-flow fluorescence measurements of 1-N^6-etheno-2-aza-ATP binding to NPM−S1 were

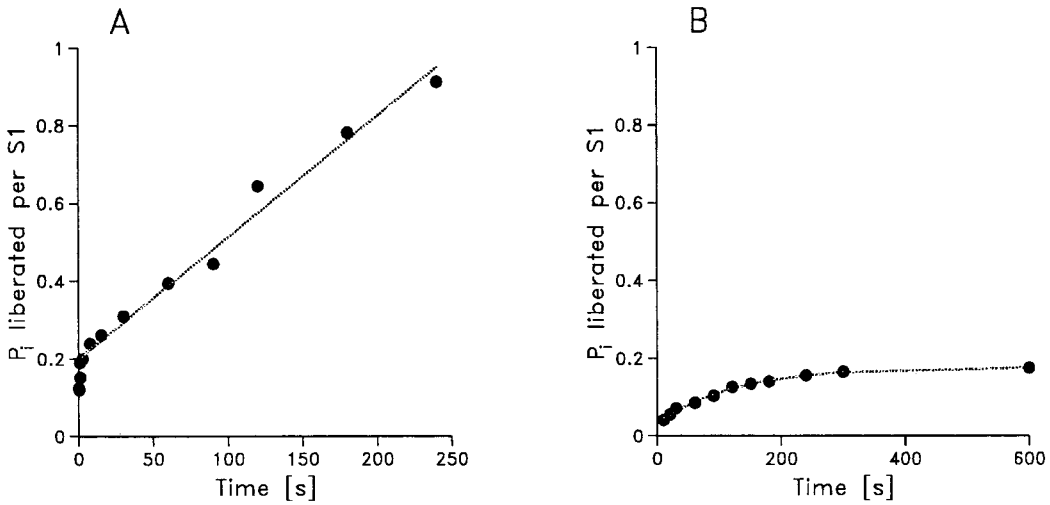

FIGURE 4: Cold-quench experiments. (A) Equal volumes of 20 μM NPM−S1 were mixed with 40 μM [γ-^{32}P]ATP and then mixed with 10 mM cold MgATP at the indicated time. After an additional 20 min, the reaction was quenched with acid. The ordinate displays the amount of radiolabeled P_i liberated per S1. (B) In a second type of experiment, 20 μM NPM−S1 was first mixed with 40 μM [γ-^{32}P]ATP and then mixed with 10 mM cold MgATP after 2−3 s, and finally the reaction was quenched with acid at the indicated time. The acid quench and determination of the fraction of ATP hydrolyzed were determined as described in Materials and Methods.

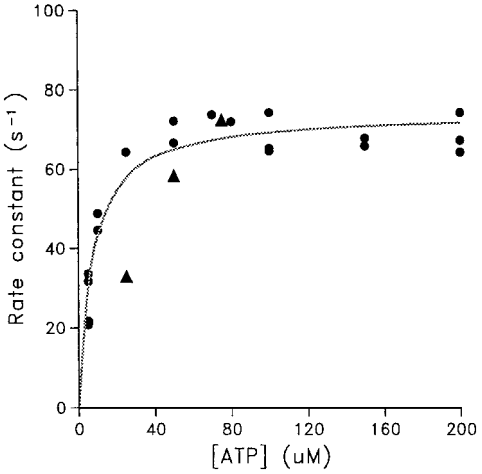

FIGURE 5: ATP concentration dependence of the rate constant of the substrate-induced fluorescence enhancement upon ATP binding to unmodified subfragment-1. Circles (●) are the observed rate constants of single-exponential fits to the fluorescence increase observed in a stopped-flow fluorimeter upon mixing 2 μM unmodified S1 with an equal volume of MgATP to obtain the indicated final concentration of MgATP. The triangles (▲) are the rate constants determined from single-turnover quench-flow experiments in which 15 μM myosin-S1 was mixed with equal volumes of MgATP to obtain the indicated final concentration of MgATP. Buffer conditions as the same as those described in the legend of Figure 1.

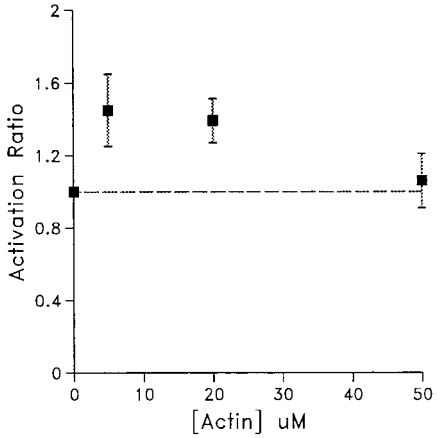

FIGURE 6: Dependence of the ATPase activity of NPM−S1 upon actin concentration. Reaction mixtures contained 1 μM NPM−S1, 50 μM ATP, 2 mM $MgCl_2$, 0.2 mM DTT, and 5 mM MOPS (pH 7.0) at 25 °C and the indicated concentration of actin. The activation ratio is defined as the ATPase rate constant in the presence of a given concentration of actin divided by the rate constant in the absence of actin.

taken to obtain an estimate of the change in the rate constant for nucleotide binding to NPM−S1 (data not shown). The observed second-order rate constant was decreased ~20-fold relative to that of unmodified S1. This is similar to the decrease observed in the second-order rate constant of ATP binding to acto-NPM−S1 as estimated from the light scattering data. This suggests that NPM modification produces similar changes in the rates of nucleotide binding to both myosin-S1 and actomyosin-S1.

Actin Activation. The ATPase activity of unmodified S1 is increased more than 100-fold by actin. One question that arises is whether the slow ATPase activity of NPM−S1 also is stimulated by actin. To explore this, the ATPase activity of NPM−S1 was measured as described in Materials and Methods, both in the presence and in the absence of different concentrations of actin. An activation ratio was defined as the ATPase activity measured in the presence of actin divided by that measured in its absence. The activation ratio data are shown in Figure 6. It is seen that the amount of actin activation is extremely small, only on the order of 45%, and is eventually followed at higher actin concentrations by actin inhibition. This is the kind of behavior typically seen when unmodified S1 hydrolyzes a nucleotide such as GTP for which the hydrolysis step is rate-limiting (*19*).

DISCUSSION

Previously, equilibrium binding studies showed two very large effects of NPM modification of myosin. The level of binding of MgATP to myosin was found to be reduced 50000-fold and that to actomyosin 10000-fold (*8*). In the work reported here, stopped-flow and quench-flow experiments were used to examine how the kinetic steps in the S1

hydrolysis mechanism scheme for NPM−S1 compare to those for unmodified myosin-S1. Here we report a third large effect, a 20000-fold decrease in the apparent rate constant of the ATP hydrolytic step, which explains the mechanism of NPM's inhibition of myosin ATP hydrolysis.

Although the rate of the ATP hydrolysis step by myosin subfragment-1 is reduced 20000-fold by NPM modification, the overall effect on the steady-state MgATP hydrolysis rate constant is only 20-fold (Table 1). For unmodified S1, the ATP hydrolysis rate constant (72 s^{-1} in Table 1) is ~1000 times faster than the measured steady-state phosphate release rate constant (0.064 s^{-1}) and the phosphate release step is rate-limiting. In the NPM-modified cycle, the single-turnover and steady-state rate constants are approximately equal (0.0038 ± 0.0004 compared to 0.0030 ± 0.0001). This indicates that the 20000-fold slower hydrolytic step is rate-limiting for NPM−S1. The rate and equilibrium constants of the ATP hydrolysis mechanisms are compared in eqs 2 (unmodified) and 3 (NPM-modified).

$$M + T \underset{10^{-5}\ s^{-1}}{\overset{4\times10^{6}\ M^{-1}\ s^{-1}}{\rightleftharpoons}} M{\cdot}T \underset{12\ s^{-1}}{\overset{60\ s^{-1}}{\rightleftharpoons}} M{\cdot}ADP{\cdot}P_i \xrightarrow{0.06\ s^{-1}} M{\cdot}ADP \overset{10^{-6}\ M}{\rightleftharpoons} M \quad (2)$$

$$M + T \underset{1.5\times10^{-2}\ s^{-1}}{\overset{2\times10^{5}\ M^{-1}\ s^{-1}}{\rightleftharpoons}} M{\cdot}T \underset{<0.0006\ s^{-1}}{\overset{0.003\ s^{-1}}{\rightleftharpoons}} M{\cdot}ADP{\cdot}P_i \xrightarrow{>0.01\ s^{-1}} M{\cdot}ADP \overset{5\times10^{-4}\ M}{\rightleftharpoons} M \quad (3)$$

The rate constants were modeled using the program Scientist (Micromath, Salt Lake City, UT) and are compatible with the quench-flow and cold-quench data. Comparison of the two schemes shows that the large reduction in the affinity constant for ATP binding to myosin is a result of changes in both the rates of ATP binding and dissociation: a 20-fold decrease in k_{+1} and a 1500-fold increase in k_{-1}.

The light scattering experiments whose results are depicted in Figures 1 and 2 show that for MgATP concentrations of <100 μM, where the dissociation of S1 from actin is clearly limited by the MgATP concentration, MgATP binds to and dissociates NPM-reacted S1 from actin 16 times more slowly than unmodified S1. This suggests that the 10000-fold decrease in the equilibrium binding constant for binding of ATP to acto-S1 caused by NPM modification is due to a 16-fold decrease in the ATP association rate constant and a 600-fold increase in the ATP dissociation rate constant for association with and dissociation from acto-S1. The aza-ATP binding data suggest a similar situation for S1 alone, about a 20-fold decrease in the nucleotide association rate.

An important consequence of the ATP hydrolysis rate constant being rate-limiting for NPM−S1 is that the predominant species in the presence of ATP will be the weakly binding S1·ATP state, rather than an equilibrium mixture of weakly binding S1·ATP and S1·ADP·P_i states, as occurs with unmodified S1 (*20*). Interestingly, the affinity of NPM-modified S1 for actin, both in the presence and in the absence of MgATP, is not very different from that of unmodified S1.

Although we have not been able to measure the rate and equilibrium constants of every step in the ATPase cycle, we have been able to determine how NPM modification affects several critical steps of the mechanism. Even though we have not directly measured the rate of dissociation of P_i and ADP from NPM−S1, enough information is available to determine how NPM modification is likely to affect these steps. Since the product of all the equilibrium constants of the hydrolysis path must be equal to the equilibrium constant for ATP hydrolysis, the 50000-fold weaker binding of ATP to NPM−S1 must be compensated for by either a more favorable equilibrium constant for the hydrolysis step or a weaker binding of products to NPM−S1. This is consistent with the observed 200−500-fold reduction in the affinity of NPM−S1 for ADP. This could be due to an increase in the rate constant of ADP dissociation, a decreased rate of ADP binding, or a combination of the two. If the effects of NPM modification upon ATP and ADP affinity are similar, then the rates of both association and dissociation would be expected to change. There must also therefore be an increase in the equilibrium constant for the hydrolysis step and/or a decreased affinity for phosphate to compensate for the much larger effect of modification upon ATP than upon ADP affinity. Available data do not allow us to distinguish between these alternatives. Single-turnover experiments (Figure 3) indicate that hydrolysis is rate-limiting for NPM−S1, but this places only lower limits on the rates of phosphate and ADP dissociation, which must be at least several times faster (>0.01 s^{-1}). We can, however, say with certainty that if the rate constant for release of P_i is reduced, it must be reduced <20-fold, since P_i release and not ATP hydrolysis would be rate-limiting, and this would be incompatible with the experiments whose results are summarized in Table 1.

Our observation that there is so little actin activation of hydrolysis of NPM−S1 suggests that the hydrolysis step is rate-limiting in the presence and absence of actin and that the product dissociation steps are not rate-limiting.

For unmodified myosin, a large fraction of the fluorescence signal change upon ATP addition is associated with the ATP hydrolysis step. The data in Figure 4 show that under conditions where substrate binding is rapid, the rates of fluorescence enhancement and hydrolysis are equal. This suggests that the hydrolysis is tightly coupled to the change in the environment of the tryptophan revealed by the fluorescence enhancement, as suggested previously (*18*).

We have found that NPM-modified S1 shows little, if any, fluorescence signal upon binding ATP. Several apparently unrelated covalent modifications of myosin-S1 such as reductive methylation of lysine residues (*15*), sulfhydryl modification (*21*), mutagenesis of critical conserved residues in the myosin active site (*22*), and some changes in substrate structure (*19*) all reduce the rate of the hydrolytic step and also reduce or eliminate the change in intrinsic fluorescence enhancement associated with substrate binding and hydrolysis by native myosin-S1. Another feature shared by these modifications is that actin activation of ATP hydrolysis is reduced and in some cases even inhibited by actin. Actin increases the rate of ATP hydrolysis by native myosin by increasing the rate of product release up to 1000-fold, but it also decreases the rate of the hydrolysis step 10−20-fold and the substrate affinity by as much as 10^4 (eq 1). The covalent modifications all have similar effects upon the kinetic mechanism as does actin in that they decrease ATP affinity, decrease the rate of the hydrolytic step, and probably increase the rate of product release. Actin can increase the rate of ATP hydrolysis of normal myosin despite slower hydrolysis by AM·ATP → AM·ADP·P_i because the slow step is circumvented in part by the dissociation of M·ATP

from actin. There is no similar pathway available for circumventing the slow hydrolysis step for the modified myosins. If the reduction in the hydrolytic rate is relatively small (SH1 modification and reductive methylation), there is a corresponding reduction in the extent of actin activation. For cases in which there is a larger inhibition of the hydrolytic rate (GTP, NPM−S1, and mutagenesis), there is a small amount of activation at low actin concentrations and inhibition at higher concentrations. A possible explanation of these observations is that there are two broad classes of myosin conformations that differ considerably in their kinetic properties. Actin and various chemical modifiers function primarily by shifting the equilibrium away from the rapidly hydrolyzing, strongly binding form (with slow product dissociation steps), characteristic of native myosin, to the slowly hydrolyzing, weakly binding form (with rapid product dissociation steps), characteristic of actomyosin and the modified myosins.

During muscle force generation, many processes occur which are more or less linked to each other. Among these many processes are the transition between the weakly binding and strongly binding forms of the myosin cross-bridge and ATP hydrolysis. One of the important questions in understanding muscle force generation is how tightly the various structural and biochemical events are coupled. The NPM-reacted cross-bridge may be useful in addressing this question because it can undergo some of the steps in the cross-bridge cycle, such as the weakly to strongly binding conformational change, quite well, but others, such as ATP hydrolysis, are inhibited. The NPM-reacted cross-bridge may thus offer the unique opportunity of isolating and studying the effect of a cross-bridge head going through just a single step within the contractile cycle, rather than the usual full complicated panoply of cross-bridge transitions.

REFERENCES

1. Lymn, R. W., and Taylor, E. W. (1971) *Biochemistry 10*, 4617−4624.
2. Stein, L. A., Schwarz, R. P., Chock, P. B., and Eisenberg, E. (1979) *Biochemistry 18*, 3895−3909.
3. Yamaguchi, M., and Sekine, T. (1966) *J. Biochem. 59*, 24−33.
4. Reisler, E., Burke, M., and Harrington, W. F. (1974) *Biochemistry 13*, 2014−2022.
5. Huston, E. E., Grammer, J. C., and Yount, R. G. (1988) *Biochemistry 27*, 8945−8952.
6. Ehrlich, A., Barnett, V. A., Chen, H. C., and Schoenberg, M. (1995) *Biochim. Biophys. Acta 1232*, 13−20.
7. Chalovich, J. M., Greene, L. E., and Eisenberg, E. (1983) *Proc. Natl. Acad. Sci. U.S.A. 80*, 4909−4913.
8. Xie, L., and Schoenberg, M. (1998) *Biochemistry 37*, 8048−8053.
9. Xu, S., Yu, L. C., and Schoenberg, M. (1998) *Biophys. J. 74*, 1110−1114.
10. Smith, S. J., and White, H. D. (1985) *J. Biol. Chem. 260*, 15146−15155.
11. Weeds, A. G., and Pope, B. (1977) *J. Mol. Biol. 111*, 129−157.
12. Pardee, J. D., and Spudich, J. A. (1982) in *Methods in Enzymology* (Fredrickson, D. W., and Cunningham, L. W., Eds.) Vol. 85, pp 164−181, Academic Press, New York.
13. Lowry, O. H., Rosebrough, N. J., Farr, A. L., and Randall, R. J. (1951) *J. Biol. Chem. 193*, 265−275.
14. Marquardt, D. W. (1963) *J. Soc. Ind. Appl. Math. 2*, 431−441.
15. White, H. D., and Rayment, I. (1993) *Biochemistry 32*, 9859−9865.
16. Dyson, R. D., and Isenberg, I. (1971) *Biochemistry 10*, 3233−3241.
17. Chalovich, J. M., Chock, P. B., and Eisenberg, E. (1981) *J. Biol. Chem. 256*, 575−578.
18. Johnson, K. A., and Taylor, E. W. (1978) *Biochemistry 17*, 3432−3442.
19. Pate, E., Franks-Skiba, K., White, H., and Cooke, R. (1993) *J. Biol. Chem. 268*, 10046−10053.
20. Taylor, E. W. (1977) *Biochemistry 16*, 732−739.
21. Ostap, E. M., White, H. D., and Thomas, D. D. (1993) *Biochemistry 32*, 6712−6720.
22. Li, X. D., Rhodes, T. E., Ikebe, R., Kambara, T., White, H., and Ikebe, M. (1998) *J. Biol. Chem. 273*, 27202−27211.

BI981778O